Structural Engineering and Mechanics, *Vol. 57, No. 2 (2016) 369-387*
DOI: http://dx.doi.org/10.12989/sem.2016.57.2.369

Homogenized thermal properties of 3D composites with full uncertainty in the microstructure

Juan Ma[*1,2], Peter Wriggers[2a] and Liangjie Li[1b]

[1]*Key Laboratory of Electronic Equipment Structure Design, Ministry of Education, Xidian University, Xi'an, 710071, P.R. China*
[2]*Institute of Continuum Mechanics, Leibniz Universität Hannover, 30167 Hannover, Germany*

(Received December 24, 2014, Revised October 26, 2015, Accepted December 17, 2015)

Abstract. In this work, random homogenization analysis for the effective thermal properties of a three-dimensional composite material with unidirectional fibers is presented by combining the equivalent inclusion method with Random Factor Method (RFM). The randomness of the micro-structural morphology and constituent material properties as well as the correlation among these random parameters are completely accounted for, and stochastic effective thermal properties as thermal expansion coefficients as well as their correlation are then sought. Results from the RFM and the Monte-Carlo Method (MCM) are compared. The impact of randomness and correlation of the micro-structural parameters on the random homogenized results is revealed by two methods simultaneously, and some important conclusions are obtained.

Keywords: random homogenization; randomness and correlation; Random Factor Method; random effective thermal proterties; Monte-Carlo Method

1. Introduction

Heterogeneous materials such as composite materials are increasingly used in different fields, e.g. the aerospace (Rong *et al.* 2015), automotive (Tian *et al.* 2015) and civil construction industries (Wu *et al.* 2014), whereby they are designed and employed to satisfy special functional requirements that conventional homogeneous materials cannot meet (Miehe *et al.* 1999). In the field of materials and mechanics, as an efficient method relating the micro-scale feature to the macro-scale response, homogenization techniques are widely used to compute the effective properties of heterogeneous materials based on the knowledge of geometry and material properties of their microstructure. These techniques are both of computational and analytical nature. For analytical techniques, early approximations for this purpose were presented by Voigt (1889) and Reuss (1929). Later, key advances were reached with the work of Eshelby (1957), Hashin and Shtrikman (1962). Additional classical models to estimate the effective properties included the self-consistent method, the Mori and Tanaka (1972) method and many others, see e.g., Aboudi

∗Corresponding author, Associate Professor, E-mail: juan@ikm.uni-hannover.de
[a]Professor, E-mail: wriggers@ikm.uni-hannover.de
[b]Master, E-mail: lilj_jiyuan@163.com

http://www.techno-press.org/?journal=sem&subpage=8 ISSN: 1225-4568 (Print), 1598-6217 (Online)

(1991), Nemat-Nasser and Hori (1999). Computational techniques based on multiscale finite element were developed as well, see e.g., Zohdi and Wriggers (2008), Stroeven *et al.* (2004).

During the manufacturing of the materials and structures, the effects of the uncertainty on the geometry and material parameters can never be avoided (Torquato 2002), and the uncertainty in material may further greatly affect the structural responses. Sometimes, the coefficient of variation of the biggest structural response was about seven times as high as that of the structural parameters (Li 1993) according to the computational results, and random structural parameters contributed more to the random dynamic response than the random external excitation (Li 1991). This recently motivated an increasing attention to random heterogeneous materials, including, e.g., composite materials with uncertainty in the location/shape of the reinforcement and/or in the pore/particle spatial distribution in the matrix as well as in the mechanical properties of the components. Many progresses about random homogenization have been reached with the work of many scholars. Sakata and coworkers (Sakata *et al.* 2008) applied the perturbation-based stochastic analysis with the equivalent inclusion method in order to estimate the influence of a geometrical uncertainty such as shape or volume fraction of inclusions on the probabilistic characteristics of a homogenized elastic property. Lu *et al.* (2013) developed a new approach to bounding effective properties of random heterogeneous materials and computed the expectation material properties for a stochastic unit cell representing the random heterogeneous materials, whereby the position of inclusions in different cells varies independently and is the only random variable. Bris (2010) overviewed a series of recent works tackling homogenization problems for some materials seen as small random perturbations of periodic materials. In addition, other different schemes used for the solution of stochastic homogenization problem were successively proposed such as multi-scale spectral stochastic method (Tootkaboni and Graham-Brady 2010), extended finite element method (Hiriyur *et al.* 2011) and many others, check Vel and Goupee (2010), Xu (2012), and effective responses of heterogeneous materials with random micro-structural properties or with random morphology as penny-shaped and slit-like random cracks were solved by these schemes.

Despite the progress made, further research is still needed on random homogenization of heterogeneous materials. The existing models mainly address the randomness of the micro-structural morphology (Torquato 2002, Lu *et al.* 2013, Hiriyur *et al.* 2011, Vel and Goupee 2010, Xu and Stefanou 2012, Knott *et al.* 2011) or sometimes of several material properties (Sakata *et al.* 2008, Tootkaboni and Graham-Brady, 2010). In particular, neither the correlations among micro-structural parameters nor the correlations among random homogenized results were ever considered in homogenization models thus far. Compared with the randomness in the microstructure, the correlation among micro-structural parameters also plays an important role to link the global properties of materials to the micro-structural feature.

Moreover, since a kind of composite material such as a fiber reinforced composite is used to bear thermal loading in (Ashida *et al.* 2003, Lascoup *et al.* 2013), a stochastic homogenization thermal analysis is really important in order to evaluate reliability of a composite structure bearing thermal stresses. Hence, a rational homogenization description of the uncertain micro-structural features and of their translation into a macroscopic, effective thermal response would well benefit the predictive capability for heterogeneous materials. From these backgrounds above, the goal of this work lies in tackling the stochastic homogenization thermal problem of composite material by a convenient approach when fully considering the uncertainty in microstructure. Herein, the Random factor method (RFM) proposed in (Ma *et al.* 2011, Gao *et al.* 2004) is extended to the computation of random effective thermal properties of a unidirectional fiber reinforced composite in three-dimension, whereby the randomness of morphology parameters and material properties of two constituents as well as the correlation among these random variables are accounted for. Furthermore, all results obtained from the RFM are compared with those from Monte-Carlo Method (MCM) in order to confirm the validity of the proposed method. Finally, the correlation in the macroscopic effective thermal properties is obtained by the MCM.

2. Stochastic homogenization for effective thermal properties of fiber-reinforced composites based on RFM

2.1 Homogenized thermal expansion coefficient tensor $\boldsymbol{\alpha}^{EI}$ of the composite materials

The equivalent inclusion method is an effective method for estimating a homogenized elastic property of composite materials. For a unidirectional fiber reinforced composite material, e.g. as shown in Fig. 1(a), an equivalent inclusion method formula based on Mori-Tanaka theory (Mori and Tanaka 1972, Tohgo 2004) can be used for such estimation. Mori-Tanaka theory is then expanded for evaluation of an effective thermal expansion coefficient of a composite material in (Takao and Taya 1985), and the homogenized effective thermal properties, that is, effective thermal expansion coefficient tensor is computed as

$$\boldsymbol{\alpha}^{EI} = \boldsymbol{\alpha}_m + V_f\,(\boldsymbol{g} + \boldsymbol{\varphi}) \tag{1}$$

where matrices $\boldsymbol{g}$ and $\boldsymbol{\varphi}$ are as follows

$$\boldsymbol{g} = \{-V_f\ (\boldsymbol{S}-\boldsymbol{I})\}^{-1}[\{\boldsymbol{I}+\boldsymbol{\beta}(\boldsymbol{E}_f-\boldsymbol{E}_m)\}^{-1}\boldsymbol{\beta}\cdot\boldsymbol{E}_f\boldsymbol{\varphi} + V_f\ (\boldsymbol{S}-\boldsymbol{I})\boldsymbol{\varphi}] = \boldsymbol{A}^{-1}[\boldsymbol{D}^{-1}\boldsymbol{\beta}\boldsymbol{E}_f - \boldsymbol{A}]\boldsymbol{\varphi} \tag{2}$$

$$\boldsymbol{\varphi} = (\boldsymbol{\alpha}_f + \boldsymbol{\alpha}_m) \tag{3}$$

In order to simplifying Eq. (2), some matrix symbols without specific physical meaning are introduced in Eq. (2) are

$$\boldsymbol{A} = -\,V_f\cdot(\boldsymbol{S}-\boldsymbol{I}),\ \ \boldsymbol{H} = (\boldsymbol{E}_f-\boldsymbol{E}_{\mathrm{m}})(\boldsymbol{S}-\boldsymbol{I})+\boldsymbol{E}_f,\ \ \boldsymbol{\beta} = \boldsymbol{A}\boldsymbol{H}^{-1},\ \ \boldsymbol{D} = \boldsymbol{I}+\boldsymbol{\beta}(\boldsymbol{E}_f-\boldsymbol{E}_m) \tag{4}$$

For an isotropic material, the elastic tensor $\boldsymbol{E}$ can be expressed as

$$\boldsymbol{E} = \frac{e(1\text{-}v)}{(1+v)(1\text{-}2v)}\begin{bmatrix} 1 & \frac{v}{1-v} & \frac{v}{1-v} & 0 & 0 & 0 \\ \frac{v}{1-v} & 1 & \frac{v}{1-v} & 0 & 0 & 0 \\ \frac{v}{1-v} & \frac{v}{1-v} & 1 & 0 & 0 & 0 \\ 0 & 0 & 0 & \frac{1-2v}{2(1-v)} & 0 & 0 \\ 0 & 0 & 0 & 0 & \frac{1-2v}{2(1-v)} & 0 \\ 0 & 0 & 0 & 0 & 0 & \frac{1-2v}{2(1-v)} \end{bmatrix} \tag{5}$$

where e is the Young's modulus of the material and v is its Poisson ratio.

S is a 6×6 matrix and depends on the shape of the inclusions. In case of long continuous

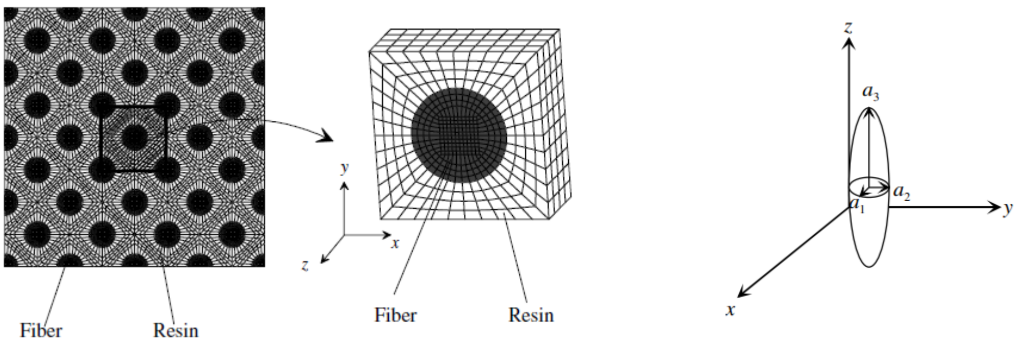

Fig. 1 (a) a unidirectional fiber reinforced plastics: periodic microstructure (left) and unit cell (right); (b): a fiber inclusion with the relationship among three geometric dimensions $a_3 >> a_{1,} a_2$

unidirectional fibers the non-zero elements of **S** are respectively:

$$S_{1111}=\frac{1}{2(1-\nu_m)}\left[\frac{a_2^2+2a_1a_2}{(a_1+a_2)^2}+(1-2\nu_m)\frac{a_2}{a_1+a_2}\right],\quad S_{1122}=\frac{1}{2(1-\nu_m)}\left[\frac{a_2^2}{(a_1+a_2)^2}-(1-2\nu_m)\frac{a_2}{a_1+a_2}\right],$$

$$S_{1212}=\frac{1}{2(1-\nu_m)}\left[\frac{a_1^2+a_2^2}{2(a_1+a_2)^2}+\frac{1-2\nu_m}{2}\right],\quad S_{1133}=\frac{1}{2(1-\nu_m)}\cdot\frac{2\nu_m a_2}{a_1+a_2},$$

$$S_{2211}=\frac{1}{2(1-\nu_m)}\left[\frac{a_1^2}{(a_1+a_2)^2}-(1-2\nu_m)\frac{a_1}{a_1+a_2}\right],\quad S_{2222}=\frac{1}{2(1-\nu_m)}\left[\frac{a_1^2+2a_1a_2}{(a_1+a_2)^2}+(1-2\nu_f)\cdot\frac{a_1}{a_1+a_2}\right],$$

$$S_{2323}=\frac{a_1}{2(a_1+a_2)},\quad S_{2233}=\frac{1}{2(1-\nu_m)}\frac{2\nu_m a_1}{a_1+a_2},\quad S_{3131}=\frac{a_2}{2(a_1+a_2)}.$$

For geometric dimensions a_1 and a_2, see Fig. 1(b). The cross-section of the fiber inclusion will be a circle if $a_1=a_2$.

2.2 Numerical characteristics of stochastic effective thermal expansion coefficient tensor

According to RFM, a random variable y can be expressed as a random factor $\widetilde{y}$ multiplied by its mean value μ_y: $y=\widetilde{y}\cdot\mu_y$. Random factor $\widetilde{y}$ represents the randomness of y, and the mean value of $\widetilde{y}$ is 1.0 and the mean square deviation of $\widetilde{y}$ is that of y. $\widetilde{y}$ and y obey the same probabilistic distribution.

In the following, RFM is explicitly applied to derive the numerical characteristics of random effective thermal expansion coefficient tensor for a unidirectional fiber reinforced composite considered, whereby Young's modulus e_m and Poisson ratio v_m of matrix, Young's modulus e_f and Poisson ratio v_f of fiber, cross-sectional dimensions of fiber a_1 and a_2, the fiber volume fraction V_f, thermal expansion coefficient of matrix and fiber α_m and α_f are random, and the correlation between e_m and v_m, e_f and v_f, a_1 and a_2 is considered as well.

These random parameters can firstly be written as $e_m=\widetilde{e}_m\cdot\mu_{e_m}$, $e_f=\widetilde{e}_f\cdot\mu_{e_f}$, $v_m=\widetilde{v}_m\cdot\mu_{v_m}$, $v_f=\widetilde{v}_f\cdot\mu_{v_f}$, $a_1=\widetilde{a}_1\cdot\mu_{a_1}$, $a_2=\widetilde{a}_2\cdot\mu_{a_2}$, $V_f=\widetilde{V}_f\cdot\mu_{v_f}$, $\alpha_m=\widetilde{\alpha}_m\cdot\mu_{\alpha_m}$, $\alpha_f=\widetilde{\alpha}_f\cdot\mu_{\alpha_f}$, where $\widetilde{e}_m$, $\widetilde{e}_f$,

$\tilde{v}_m$, $\tilde{v}_f$, $\tilde{a}_1$, $\tilde{a}_2$, $\tilde{V}_f$, $\tilde{\alpha}_m$ and $\tilde{\alpha}_f$ are random factors of the random parameters. The mean values of the parameters are μ_{e_m}, μ_{e_f}, μ_{v_m}, μ_{v_f}, μ_{a_1}, μ_{a_2}, μ_{V_f}, μ_{α_m} and μ_{α_f}. The mean values of these random factors are 1.0, and the mean square deviations are σ_{e_m}, σ_{e_f}, σ_{v_m}, σ_{v_f}, σ_{a_1}, σ_{a_2}, σ_{V_f}, σ_{α_m}, σ_{α_f} for both random parameters and random factors.

To obtain the coefficient of variance of $\boldsymbol{\alpha}^{EI}$, mean value and mean square deviation of $\boldsymbol{\alpha}^{EI}$ should be firstly computed. From Eqs. (1)-(5), matrices $\boldsymbol{A}$, $\boldsymbol{H}$, $\boldsymbol{\beta}$, $\boldsymbol{D}$, $\boldsymbol{g}$ and tensor $\boldsymbol{\alpha}^{EI}$ are functions of parameters e_m, e_f, v_m, v_f, a_1, a_2, V_f, α_m and α_f. The method of computing mean value is essentially equivalent to a deterministic evaluation of the effective thermal expansion coefficient tensor by RFM, that is, mean values of $\boldsymbol{A}$, $\boldsymbol{H}$, $\boldsymbol{\beta}$, $\boldsymbol{D}$, $\boldsymbol{g}$ and $\boldsymbol{\alpha}^{EI}$ can be obtained by simply substituting the mean values μ_{e_m}, μ_{e_f}, μ_{v_m}, μ_{v_f}, μ_{a_1}, μ_{a_2}, μ_{V_f}, μ_{α_m}, μ_{α_f} into Eqs. (1)-(5) according to the random variables' moment method (Ma *et al.* 2011, Gao *et al.* 2004). Hence, attention will be focused to the evaluation of the mean square deviation of $\boldsymbol{\alpha}^{EI}$.

$\boldsymbol{\alpha}^{EI}$ can firstly be rewritten as

$$\boldsymbol{\alpha}^{EI} = \boldsymbol{\alpha}_m + V_f(\boldsymbol{g} + \boldsymbol{\varphi}) = \boldsymbol{\alpha}^{EI}(e_m, e_f, v_m, v_f, a_1, a_2, V_f, \alpha_m, \alpha_f) \tag{6}$$

From Eq. (6) and by random variables' moment method, the mean square deviation $\sigma_{\boldsymbol{\alpha}^{EI}}$ of effective thermal expansion coefficient tensor $\boldsymbol{\alpha}^{EI}$ without considering the correlation existing in the random parameters is

$$\begin{aligned}\sigma_{\boldsymbol{\alpha}^{EI}} = \{ & (\frac{\partial \boldsymbol{\alpha}^{EI}}{\partial e_m})^2 \sigma_{e_m}^2 + (\frac{\partial \boldsymbol{\alpha}^{EI}}{\partial v_m})^2 \sigma_{v_m}^2 + (\frac{\partial \boldsymbol{\alpha}^{EI}}{\partial e_f})^2 \sigma_{e_f}^2 + (\frac{\partial \boldsymbol{\alpha}^{EI}}{\partial v_f})^2 \sigma_{v_f}^2 + (\frac{\partial \boldsymbol{\alpha}^{EI}}{\partial a_1})^2 \sigma_{a_1}^2 + \\ & (\frac{\partial \boldsymbol{\alpha}^{EI}}{\partial a_2})^2 \sigma_{a_2}^2 + (\frac{\partial \boldsymbol{\alpha}^{EI}}{\partial V_f})^2 \sigma_{V_f}^2 + (\frac{\partial \boldsymbol{\alpha}^{EI}}{\partial \alpha_m})^2 \sigma_{\alpha_m}^2 + (\frac{\partial \boldsymbol{\alpha}^{EI}}{\partial \alpha_f})^2 \sigma_{\alpha_f}^2 \}^{\frac{1}{2}}\end{aligned} \tag{7}$$

Mean square deviation $\sigma_{\boldsymbol{\alpha}^{EI}}$ of $\boldsymbol{\alpha}^{EI}$ fully considering the correlation among random parameters is

$$\begin{aligned}\sigma_{\boldsymbol{\alpha}^{EI}} = \{ & (\frac{\partial \boldsymbol{\alpha}^{EI}}{\partial e_m})^2 \sigma_{e_m}^2 + (\frac{\partial \boldsymbol{\alpha}^{EI}}{\partial v_m})^2 \sigma_{v_m}^2 + (\frac{\partial \boldsymbol{\alpha}^{EI}}{\partial e_f})^2 \sigma_{e_f}^2 + (\frac{\partial \boldsymbol{\alpha}^{EI}}{\partial v_f})^2 \sigma_{v_f}^2 + (\frac{\partial \boldsymbol{\alpha}^{EI}}{\partial a_1})^2 \sigma_{a_1}^2 + \\ & (\frac{\partial \boldsymbol{\alpha}^{EI}}{\partial a_2})^2 \sigma_{\alpha_2}^2 \; (\frac{\partial \boldsymbol{\alpha}^{EI}}{\partial V_f})^2 \sigma_{V_f}^2 + (\frac{\partial \boldsymbol{\alpha}^{EI}}{\partial \alpha_m})^2 \sigma_{\alpha_m}^2 + (\frac{\partial \boldsymbol{\alpha}^{EI}}{\partial \alpha_f})^2 \sigma_{\alpha_f}^2 + (\frac{\partial \boldsymbol{\alpha}^{EI}}{\partial e_m} \cdot \frac{\partial \boldsymbol{\alpha}^{EI}}{\partial v_m}) \cdot \sigma_{e_m} \cdot \sigma_{v_m} \cdot \rho_{e_m v_m} \\ & + (\frac{\partial \boldsymbol{\alpha}^{EI}}{\partial e_f} \cdot \frac{\partial \boldsymbol{\alpha}^{EI}}{\partial v_f}) \cdot \sigma_{e_f} \cdot \sigma_{v_f} \cdot \rho_{e_f v_f} + (\frac{\partial \boldsymbol{\alpha}^{EI}}{\partial a_1} \cdot \frac{\partial \boldsymbol{\alpha}^{EI}}{\partial a_2}) \cdot \sigma_{a_1} \cdot \sigma_{a_2} \cdot \rho_{a_1 a_2} \}^{\frac{1}{2}}\end{aligned} \tag{8}$$

where $\rho_{e_m v_m}$, $\rho_{e_f v_f}$ and $\rho_{a_1 a_2}$ are correlation coefficients of e_m and v_m, e_f and v_f, a_1 and a_2, respectively.

The explicit expressions of the partial derivatives $\frac{\partial \boldsymbol{\alpha}^{EI}}{\partial e_m}$, $\frac{\partial \boldsymbol{\alpha}^{EI}}{\partial v_m}$, $\frac{\partial \boldsymbol{\alpha}^{EI}}{\partial e_f}$, $\frac{\partial \boldsymbol{\alpha}^{EI}}{\partial v_f}$, $\frac{\partial \boldsymbol{\alpha}^{EI}}{\partial a_1}$, $\frac{\partial \boldsymbol{\alpha}^{EI}}{\partial a_2}$,

$\frac{\partial \boldsymbol{\alpha}^{EI}}{\partial V_f}$, $\frac{\partial \boldsymbol{\alpha}^{EI}}{\partial \alpha_m}$ and $\frac{\partial \boldsymbol{\alpha}^{EI}}{\partial \alpha_f}$ in Eqs. (7)-(8) are all derived similarly. For conciseness, only the partial derivative $\frac{\partial \boldsymbol{\alpha}^{EI}}{\partial \nu_f}$ is explicitly analyzed (the formulations of other partial derivatives are listed as Eqs. (1)-(8) in Appendix). The application of the overall approach to the remaining partial derivatives follows in a straightforward fashion from the methods employed in $\frac{\partial \boldsymbol{\alpha}^{EI}}{\partial \nu_f}$. From Eqs. (1)-(4) and derivation rule, $\frac{\partial \boldsymbol{\alpha}^{EI}}{\partial \nu_f}$ can be expressed as

$$\begin{aligned}\frac{\partial \boldsymbol{\alpha}^{EI}}{\partial \nu_f} &= V_f\{\frac{\partial \boldsymbol{A}^{-1}}{\partial \nu_f}(\boldsymbol{D}^{-1}\boldsymbol{\beta}\boldsymbol{E}_f - \boldsymbol{A})\boldsymbol{\varphi} + \boldsymbol{A}^{-1}(\frac{\partial \boldsymbol{D}^{-1}}{\partial \nu_f}\boldsymbol{\beta}\boldsymbol{E}_f + \boldsymbol{D}^{-1}\frac{\partial \boldsymbol{\beta}}{\partial \nu_f}\boldsymbol{E}_f + \boldsymbol{D}^{-1}\boldsymbol{\beta}\frac{\partial \boldsymbol{E}_f}{\partial \nu_f} - \frac{\partial \boldsymbol{A}}{\partial \nu_f})\boldsymbol{\varphi}\} \\ &= V_f\frac{\partial \boldsymbol{A}^{-1}}{\partial \nu_f}(\boldsymbol{D}^{-1}\boldsymbol{\beta}\boldsymbol{E}_f - \boldsymbol{A})\boldsymbol{\varphi} + V_f\boldsymbol{A}^{-1}\frac{\partial \boldsymbol{D}^{-1}}{\partial \nu_f}\boldsymbol{\beta}\boldsymbol{E}_f\boldsymbol{\varphi} + V_f\boldsymbol{A}^{-1}\boldsymbol{D}^{-1}\frac{\partial \boldsymbol{\beta}}{\partial \nu_f}\boldsymbol{E}_f\boldsymbol{\varphi} + V_f\boldsymbol{A}^{-1}\boldsymbol{D}^{-1} \\ &\quad \cdot\boldsymbol{\beta}\frac{\partial \boldsymbol{E}_f}{\partial \nu_f}\boldsymbol{\varphi} - V_f\boldsymbol{A}^{-1}\frac{\partial \boldsymbol{A}}{\partial \nu_f}\boldsymbol{\varphi}\end{aligned} \tag{9}$$

Once again, for conciseness only computation of the first term $V_f\frac{\partial \boldsymbol{A}^{-1}}{\partial \nu_f}(\boldsymbol{D}^{-1}\boldsymbol{\beta}\boldsymbol{E}_f - \boldsymbol{A})\boldsymbol{\varphi}$ is analyzed hereafter in detailed, as the other four terms in Eq. (9) are computed in analogous way. In this term, only $\frac{\partial \boldsymbol{A}^{-1}}{\partial \nu_f}$ is a function of ν_f, whereas $\boldsymbol{D}^{-1}$, $\boldsymbol{\beta}$, $\boldsymbol{E}_f$, $\boldsymbol{A}$ and $\boldsymbol{\varphi}$ are constant matrices obtained by attributing to the nine random parameters their mean values. In order to compute $\frac{\partial \boldsymbol{A}^{-1}}{\partial \nu_f}$, the mean values of all parameters except for ν_f are first inserted into the matrices $\boldsymbol{A}^{-1}$, then the derivative with respect to ν_f is computed, and finally the mean value of ν_f is substituted.

Completely analogous procedures are used to compute the other four terms in Eq. (9), $V_f\boldsymbol{A}^{-1}\frac{\partial \boldsymbol{D}^{-1}}{\partial \nu_f}\boldsymbol{\beta}\boldsymbol{E}_f\ \boldsymbol{\varphi}$, $V_f\boldsymbol{A}^{-1}\boldsymbol{D}^{-1}\frac{\partial \boldsymbol{\beta}}{\partial \nu_f}\boldsymbol{E}_f\ \boldsymbol{\varphi}$, $V_f\boldsymbol{A}^{-1}\boldsymbol{D}^{-1}\boldsymbol{\beta}\frac{\partial \boldsymbol{E}_f}{\partial \nu_f}\ \boldsymbol{\varphi}$ and $V_f\boldsymbol{A}^{-1}\frac{\partial \boldsymbol{A}}{\partial \nu_f}\ \boldsymbol{\varphi}$. Hence, the partial derivative $\frac{\partial \boldsymbol{\alpha}^{EI}}{\partial \nu_f}$ in Eqs. (7)-(8) is obtained. All the other partial derivatives $\frac{\partial \boldsymbol{\alpha}^{EI}}{\partial e_m}$, $\frac{\partial \boldsymbol{\alpha}^{EI}}{\partial \nu_m}$, $\frac{\partial \boldsymbol{\alpha}^{EI}}{\partial e_f}$, $\frac{\partial \boldsymbol{\alpha}^{EI}}{\partial a_1}$, $\frac{\partial \boldsymbol{\alpha}^{EI}}{\partial a_2}$, $\frac{\partial \boldsymbol{\alpha}^{EI}}{\partial V_f}$, $\frac{\partial \boldsymbol{\alpha}^{EI}}{\partial \alpha_m}$ and $\frac{\partial \boldsymbol{\alpha}^{EI}}{\partial \alpha_f}$ in Eqs. (7)-(8) can be computed in the same way, and the mean square deviation $\sigma_{\boldsymbol{\alpha}^{EI}}$ of $\boldsymbol{\alpha}^{EI}$ can finally be acquired. The coefficient of variance of $\boldsymbol{\alpha}^{EI}$ is thus

$$\gamma_{\boldsymbol{\alpha}^{EI}} = \frac{\sigma_{\boldsymbol{\alpha}^{EI}}}{\mu_{\boldsymbol{\alpha}^{EI}}} \tag{10}$$

Table 1 Mean values of random parameters of fiber and matrix

	e (GPa)	v	α ($\times10^{-6}$ 1/K)	a_1 (mm)	a_2 (mm)
Fiber (E-glass)	e_f=73.0	v_f=0.2156	α_f=5.0	0.04	0.05
Matrix (Epoxy)	e_m =4.5	v_m =0.39	α_m =81.0		

Table 2 10 samples of random parameters e_m, v_m, a_1 and a_2 when $\gamma_{e_m}=\gamma_{v_m}=\gamma_{a_1}=\gamma_{a_2}$ =0.05

$\rho_{e_m v_m}$ =0		$\rho_{a_1 a_2}$ =0		$\rho_{e_m v_m}$ =0.5		$\rho_{a_1 a_2}$ =0.5		$\rho_{e_m v_m}$ =1		$\rho_{a_1 a_2}$ =1	
e_m ($\times10^9$)	v_m	a_1 ($\times10^{-3}$)	a_2 ($\times10^{-3}$)	e_m ($\times10^9$)	v_m	a_1 ($\times10^{-3}$)	a_2 ($\times10^{-3}$)	e_m ($\times10^9$)	v_m	a_1 ($\times10^{-3}$)	a_2 ($\times10^{-3}$)
4.6210	0.3637	0.4974	0.3827	4.6210	0.3724	0.4974	0.3840	4.6210	0.4005	0.4974	0.3980
4.9126	0.4492	0.4940	0.4015	4.9126	0.4591	0.4940	0.3989	4.9126	0.4258	0.4940	0.3952
3.9918	0.4041	0.5080	0.3757	3.9918	0.3802	0.5080	0.3822	3.9918	0.3460	0.5080	0.4064
4.6940	0.3888	0.5078	0.3777	4.6940	0.3973	0.5078	0.3838	4.6940	0.4068	0.5078	0.4063
4.5717	0.4039	0.4784	0.3999	4.5717	0.4052	0.4784	0.3912	4.5717	0.3962	0.4784	0.3827
4.2058	0.3860	0.4992	0.4307	4.2058	0.3738	0.4992	0.4262	4.2058	0.3645	0.4992	0.3994
4.4024	0.3876	0.4959	0.3846	4.4024	0.3837	0.4959	0.3850	4.4024	0.3815	0.4959	0.3967
4.5771	0.4190	0.5157	0.4074	4.5771	0.4185	0.5157	0.4127	4.5771	0.3967	0.5157	0.4126
5.3051	0.4175	0.5273	0.3955	5.3051	0.4487	0.5273	0.4070	5.3051	0.4598	0.5273	0.4219
5.1231	0.4176	0.5277	0.4223	5.1231	0.4409	0.5277	0.4304	5.1231	0.4440	0.5277	0.4222

where $\mu_{\boldsymbol{\alpha}^{EI}}$ is the mean value of $\boldsymbol{\alpha}^{EI}$, $\sigma_{\boldsymbol{\alpha}^{EI}}$ is the mean square deviation of $\boldsymbol{\alpha}^{EI}$ computed with Eqs. (7)-(8).

3. Numerical example

Hereafter, for a unidirectional fiber reinforced plastic composites with fiber in Fig. 1, the coefficients of variance of $\boldsymbol{\alpha}^{EI}$ caused by microscopic uncertainty are inspected with the RFM-based homogenization analysis. The mean values of the random micro-structural parameters, including the material properties and thermal parameters of the constituents (E-Glass fibers and epoxy matrix) and the cross-sectional dimensions of the fibers are listed in Table 1. In order to validate the proposed method, the RFM results are compared with those of the MCM. Unless otherwise specified, the mean value of V_f is assumed as 0.25 and the number of simulation by MCM is 10000.

Based on the Cholesky factorization of covariance matrix of random vector (Touran and Wiser, 1992), the simulation of the correlation among random micro-structural parameters is realized by MCM in this work. According to the mean value of all random parameters in Table 1, their samples obeying normal distribution and satisfying different correlative conditions can be generated by MCM. The samples of random parameters e_m, v_m, a_1 and a_2 with different correlative cases are listed in Table 2 and illustrated in Fig. 2.

Clearly, when $\rho_{e_m v_m}$ =1 or $\rho_{a_1 a_2}$ =1, the relationship between e_m and v_m, a_1 and a_2 is perfectly positive correlative, points corresponding to e_m and v_m, a_1 and a_2 are in a straight line. Moreover,

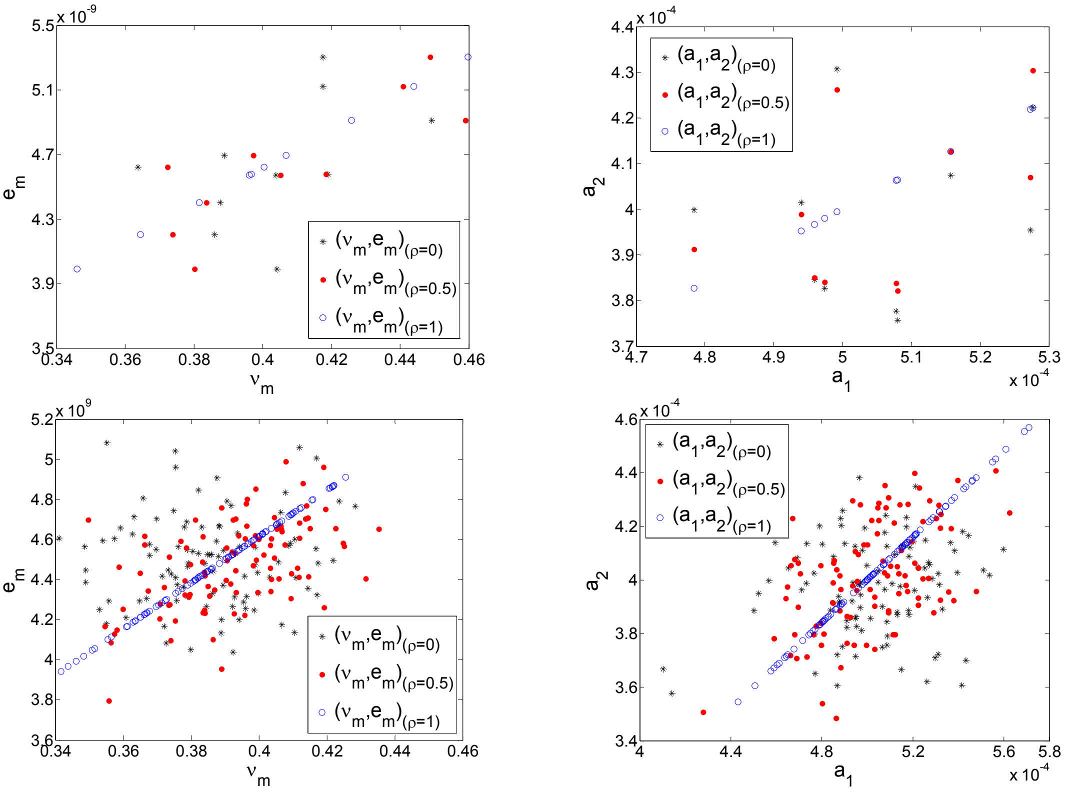

Fig. 2 Distribution of 10 samples corresponding to Table 2 (above) and of 100 samples (below) for different values of ρ

the larger the correlation coefficients $\rho_{e_m v_m}$ or $\rho_{a_1 a_2}$, the closer the points of samples satisfying $\rho_{e_m v_m}$ or $\rho_{a_1 a_2}$ to that straight line. In the following sections 3.1-3.4, samples of parameters satisfying different correlative cases are used in the simulation by MCM, and the correlation among random effective properties is examined as well.

3.1 Effects of the randomness of micro-structural parameters on the randomness of $\boldsymbol{\alpha}^{EI}$

Mean square deviations $\sigma_{\boldsymbol{\alpha}^{EI}}$ and variation coefficients $\gamma_{\boldsymbol{\alpha}^{EI}}$ of $\boldsymbol{\alpha}^{EI}$ obtained from both the RFM and MCM are listed in Table 3 considering the randomness of each micro-structural parameter in turn.

First of all, Table 3 shows that RFM and MCM results are in very good mutual agreement, which validates the proposed RFM procedure. Moreover, from Table 3 it emerges that the effect of every random parameter on the randomness of $\boldsymbol{\alpha}^{EI}$ is very different, especially every element of $\boldsymbol{\alpha}^{EI}$ more greatly affected by every random parameter is quite different. The relationship, however, between coefficients of variance of random parameters and random effective results is basically linear, so here only the curves of α_m and V_f are illustrated as instances in Fig. 3. According to the statistical results here, among all of random parameters, the randomness of α_m has the greatest effect on that of $\boldsymbol{\alpha}^{EI}$; and the randomness of V_f takes the second place and affects main diagonal elements α_1 and α_2 of $\boldsymbol{\alpha}^{EI}$ more greatly; the randomness of v_m takes the third place with a greater effect on element α_2; the fourth is the randomness of e_m and e_f as well as α_1 and α_2, and the former influences element α_3 clearly while the latter has a greater impact on α_1 and α_2; the last group is v_f and α_f with obvious effects on elements α_2 and α_3, respectively. Moreover, the randomness of v_f, e_m, e_f, a_1 and a_2 respectively has no impact on the randomness of elements α_1, α_2, α_2, α_3 and α_3.

3.2 Impacts of the correlation among micro-structural parameters on $\boldsymbol{\alpha}^{EI}$

When considering the randomness of all micro-structural parameters simultaneously and the coefficient of variance is $\gamma_{e_m}=\gamma_{v_m}=\gamma_{e_f}=\gamma_{v_f}=\gamma_{a_1}=\gamma_{a_2}=\gamma_{V_f}=\gamma_{\alpha_m}=\gamma_{\alpha_f}$, mean square deviation $\sigma_{\boldsymbol{\alpha}^{EI}}$ and coefficients of variance $\gamma_{\boldsymbol{\alpha}^{EI}}$ of $\boldsymbol{\alpha}^{EI}$ are listed in Tables 4-5 and illustrated in Fig. 4. Here V_f=0.25 and the simulation number is 10000.

Table 3 Mean square deviations and variation coefficients of $\boldsymbol{\alpha}^{EI}$ when V_f=0.25

	Results obtained from RFM						Results obtained from MCM (10000)					
	σ_{α_1} ($\times10^{-6}$)	σ_{α_2} ($\times10^{-6}$)	σ_{α_3} ($\times10^{-6}$)	γ_{α_1} ($\times10^{-3}$)	γ_{α_2} ($\times10^{-3}$)	$\gamma_{\alpha 3}$ ($\times10^{-3}$)	σ_{α_1} ($\times10^{-6}$)	σ_{α_2} ($\times10^{-6}$)	σ_{α_3} ($\times10^{-6}$)	γ_{α_1} ($\times10^{-3}$)	γ_{α_2} ($\times10^{-3}$)	$\gamma_{\alpha 3}$ ($\times10^{-3}$)
γ_{em}=0.05	0.0333	0.0054	0.5861	0.3030	0.0519	3.8305	0.0332	0.0054	0.5828	0.3020	0.0520	3.8090
γ_{v_m}=0.05	0.0817	0.4382	0.1669	0.7435	4.2109	1.0909	0.0807	0.4378	0.1967	0.7342	4.2078	1.2860
γ_{e_f}=0.05	0.0332	0.0055	0.5862	0.3023	0.0526	3.8310	0.0334	0.0054	0.5850	0.3038	0.0523	3.8238
γ_{v_f}=0.05	0.0004	0.1706	0.0487	0.0039	1.6400	0.3184	0.0004	0.1699	0.0484	0.0036	1.6331	0.3163
γ_{a_1}=0.05	0.3550	0.2600	0.0075	3.2305	2.4987	0.0490	0.3572	0.2639	0.0085	3.2510	2.5360	0.0556
γ_{a_2}=0.05	0.3560	0.2600	0.0080	3.2396	2.4987	0.0523	0.3555	0.2594	0.0085	3.2351	2.4931	0.0554
γ_{V_f}=0.05	1.2669	1.1207	0.7738	11.529	10.771	5.0568	1.2599	1.1148	0.7719	11.464	10.712	5.0449
γ_{α_m}=0.05	5.4104	5.1358	7.4415	49.235	49.356	48.633	5.3825	5.1092	7.4029	48.933	49.052	48.334
γ_{α_f}=0.05	0.0840	0.0670	0.2094	0.7642	0.6441	1.3682	0.0835	0.0667	0.2083	0.7603	0.6408	1.3610

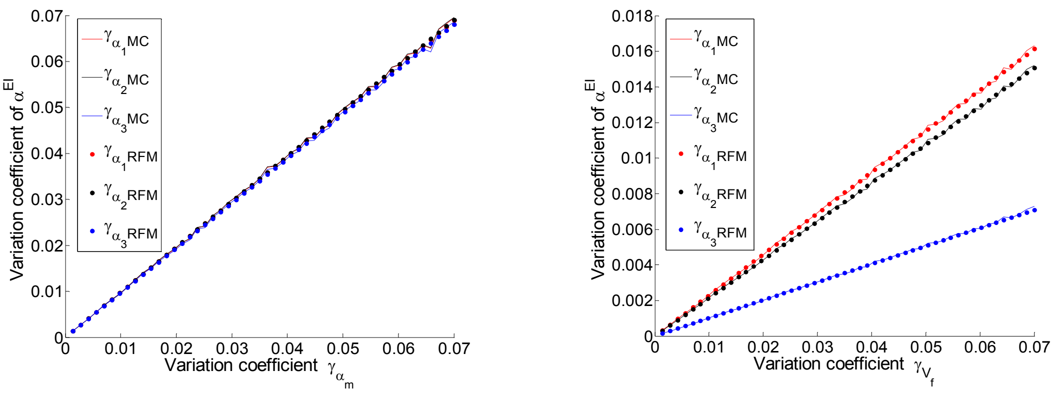

Fig. 3 Variation of the randomness of $\boldsymbol{\alpha}^{EI}$ with the randomness of α_m (left) and V_f (right)

Table 4 $\sigma_{\boldsymbol{\alpha}^{EI}}$ and $\gamma_{\boldsymbol{\alpha}^{EI}}$ of $\boldsymbol{\alpha}^{EI}$ under different correlative cases when γ=0.05 and V_f=0.25 γ_{α_1}

	Results of Random Factor Method						Results of Monte-Carlo Method (MCM: 10000)					
	σ_{α_1} ($\times 10^{-5}$)	σ_{α_2} ($\times 10^{-5}$)	σ_{α_3} ($\times 10^{-5}$)	γ_{α_1} ($\times 10^{-2}$)	γ_{α_2} ($\times 10^{-2}$)	$\gamma_{\alpha 3}$ ($\times 10^{-2}$)	σ_{α_1} ($\times 10^{-5}$)	σ_{α_2} ($\times 10^{-5}$)	σ_{α_3} ($\times 10^{-5}$)	γ_{α_1} ($\times 10^{-2}$)	γ_{α_2} ($\times 10^{-2}$)	$\gamma_{\alpha 3}$ ($\times 10^{-2}$)
ρ =0	0.558	0.5291	0.7532	5.0788	5.0847	4.9225	0.5580	0.5290	0.7533	5.0784	5.0844	4.9222
ρ =0.5	0.5575	0.5288	0.7536	5.0736	5.0817	4.9254	0.5573	0.5286	0.7538	5.0735	5.0815	4.9252
$\rho_{e_m v_m}$ =0.5	0.5581	0.5291	0.7537	5.0790	5.0849	4.9259	0.5581	0.5290	0.7536	5.0786	5.0847	4.9256
$\rho_{e_f v_f}$ =0.5	0.5581	0.5291	0.7534	5.0789	5.0848	4.9235	0.5580	0.5291	0.7535	5.0786	5.0845	4.9234
$\rho_{a_1 a_2}$ =0.5	0.5575	0.5288	0.7532	5.0735	5.0816	4.9225	0.5573	0.5285	0.7533	5.0731	5.0814	4.9223

Here ρ means $\rho_{e_m v_m} = \rho_{e_f v_f} = \rho_{a_1 a_2}$, γ means $\gamma_{e_m} = \gamma_{v_m} = \gamma_{e_f} = \gamma_{v_f} = \gamma_{a_1} = \gamma_{a_2} = \gamma_{V_f} = \gamma_{\alpha_m} = \gamma_{\alpha_f}$.

Table 5 $\sigma_{\boldsymbol{\alpha}^{EI}}$ and $\gamma_{\boldsymbol{\alpha}^{EI}}$ of $\boldsymbol{\alpha}^{EI}$ under different random and correlative conditions

	Results of RFM						Results of MCM (MCM: 10000)					
	σ_{α_1} ($\times 10^{-5}$)	σ_{α_2} ($\times 10^{-5}$)	σ_{α_3} ($\times 10^{-5}$)	γ_{α_1} ($\times 10^{-2}$)	γ_{α_2} ($\times 10^{-2}$)	γ_{α_3} ($\times 10^{-2}$)	σ_{α_1} ($\times 10^{-5}$)	σ_{α_2} ($\times 10^{-5}$)	σ_{α_3} ($\times 10^{-5}$)	γ_{α_1} ($\times 10^{-2}$)	γ_{α_2} ($\times 10^{-2}$)	γ_{α_3} ($\times 10^{-2}$)
γ =0.05, ρ =0	0.5581	0.5291	0.7532	5.0788	5.0847	4.9225	0.5580	0.5290	0.7533	5.0784	5.0844	4.9222
γ =0.05, ρ =0.8	0.5572	0.5286	0.7539	5.0706	5.0800	4.9270	0.5573	0.5283	0.7542	5.0702	5.0805	4.9273
γ =0.1, ρ =0	1.1162	1.0582	1.5064	10.158	10.169	9.8451	1.1162	1.0582	1.5066	10.157	10.167	9.8449
γ =0.1, ρ =0.8	1.1144	1.0572	1.5078	10.141	10.157	9.8538	1.1146	1.0571	1.5080	10.140	10.159	9.8535

Here γ means $\gamma_{e_m} = \gamma_{v_m} = \gamma_{e_f} = \gamma_{v_f} = \gamma_{V_f} = \gamma_{a_1} = \gamma_{a_2} = \gamma_{\alpha_m} = \gamma_{\alpha_f}$, ρ means $\rho_{e_m v_m} = \rho_{e_f v_f} = \rho_{a_1 a_2}$.

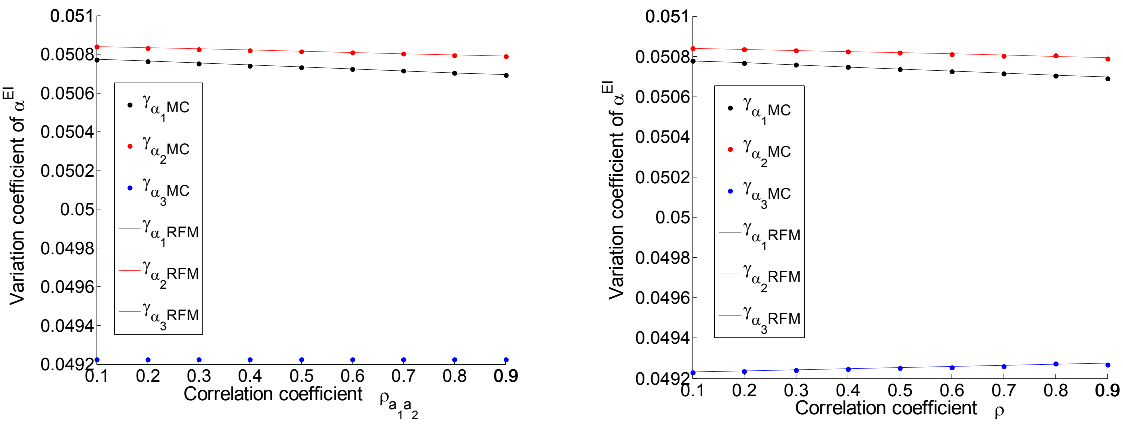

Fig. 4 Variation of the randomness of $\boldsymbol{\alpha}^{EI}$ with $\rho_{a_1 a_2}$ (left) and with $\rho = \rho_{e_m v_m} = \rho_{e_f v_f} = \rho_{a_1 a_2}$ (right)

Tables 4-5 and Fig. 4 interestingly demonstrate the interactive effects due to the simultaneous variability of different random parameters. The coefficient of variance $\gamma_{\boldsymbol{\alpha}^{EI}}$ in Tables 4-5 is much larger than those in Table 3, which shows that the randomness of each element of $\boldsymbol{\alpha}^{EI}$ is an interactive and complementary result from the effects of all parameters. Secondly, when

Table 6 Variation coefficients $\gamma_{\boldsymbol{\alpha}^{EI}}$ of α^{EI} under different correlative conditions (RFM)

	ρ								
	0.1	0.2	0.3	0.4	0.5	0.6	0.7	0.8	0.9
γ_{α_1} ($\times10^{-2}$)	5.0778	5.0768	5.0758	5.0747	5.0736	5.0727	5.0717	5.0706	5.0697
$\hat{\gamma}_{\alpha_1}$ ($\times10^{-2}$)	5.0788	5.0788	5.0788	5.0788	5.0788	5.0788	5.0788	5.0788	5.0788
γ_{α_2} ($\times10^{-2}$)	5.0841	5.0835	5.0829	5.0824	5.0817	5.0812	5.0806	5.0800	5.0794
$\hat{\gamma}_{\alpha_2}$ ($\times10^{-2}$)	5.0847	5.0847	5.0847	5.0847	5.0847	5.0847	5.0847	5.0847	5.0847
γ_{α_3} ($\times10^{-2}$)	4.9231	4.9236	4.9242	4.9247	4.9254	4.9258	4.9264	4.9270	4.9275
$\hat{\gamma}_{\alpha_3}$ ($\times10^{-2}$)	4.9225	4.9225	4.9225	4.9225	4.9225	4.9225	4.9225	4.9225	4.9225

Here ρ means $\rho_{e_m v_m} = \rho_{e_f v_f} = \rho_{a_1 a_2}$, $\gamma_{\boldsymbol{\alpha}^{EI}}$ and $\hat{\gamma}_{\boldsymbol{\alpha}^{EI}}$ are coefficients of variance when $\rho\neq0$ and $\rho=0$.

Table 7 Coefficients of variance of $\boldsymbol{\alpha}^{EI}$ under different V_f and ρ (MCM: 10000)

		V_f								
		0.1	0.2	0.3	0.4	0.5	0.6	0.7	0.8	0.9
ρ=0.4	γ_{α_1} ($\times10^{-2}$)	5.0082	5.0531	5.0937	5.1225	5.1405	5.1505	5.1549	5.1558	5.1546
ρ=0	$\hat{\gamma}_{\alpha_1}$ ($\times10^{-2}$)	5.0101	5.0568	5.0979	5.1264	5.1437	5.1527	5.1562	5.1564	5.1548
ρ=0.6	γ_{α_2} ($\times10^{-2}$)	5.0065	5.0531	5.1098	5.1649	5.2145	5.2582	5.2970	5.3327	5.3669
ρ=0	$\hat{\gamma}_{\alpha_2}$ ($\times10^{-2}$)	5.0077	5.0560	5.1137	5.1690	5.2182	5.2610	5.2989	5.3336	5.3672
ρ=0.9	γ_{α_3} ($\times10^{-2}$)	5.0825	4.9577	4.9076	4.8845	4.8724	4.8655	4.8613	4.8586	4.8568
ρ=0	$\hat{\gamma}_{\alpha_3}$ ($\times10^{-2}$)	5.0652	4.9503	4.9042	4.8829	4.8716	4.8651	4.8611	4.8585	4.8568

Here ρ means $\rho_{e_m v_m} = \rho_{e_f v_f} = \rho_{a_1 a_2}$.

considering the randomness of all parameters simultaneously, $\gamma_{\boldsymbol{\alpha}^{EI}}$ significantly increases when variation coefficient of parameters changes from 0.05 to 0.1 as shown in Table 5. Moreover, coefficient of variance $\gamma_{\boldsymbol{\alpha}^{EI}}$ obtained considering the correlation among all random parameters is different from that obtained not considering or only partly considering this correlation, which again indicates a complementary and interactive effect of $\rho_{e_m v_m}$, $\rho_{a_1 a_2}$ and $\rho_{e_f v_f}$ on the random homogenized results. For example, γ_{α_3} slightly increase with the increasing $\rho_{e_m v_m}$ or $\rho_{e_f v_f}$, but it nearly remains a constant with the augmenting $\rho_{a_1 a_2}$. As a result, γ_{α_3} goes up slightly with increasing $\rho_{e_m v_m} = \rho_{e_f v_f} = \rho_{a_1 a_2}$.

When all micro-structural parameters are random and the correlation among random parameters is considered completely, coefficient of variance of $\boldsymbol{\alpha}^{EI}$ under different correlative conditions is displayed in Table 6 by RFM. Once again, with the increase of ρ, the correlation among random parameters strengthens the randomness of α_3 but weaken the randomness of α_1 and α_2 as illustrated in Fig. 4.

3.3 Influences of V_f on the randomness of $\boldsymbol{\alpha}^{EI}$

Geometry of a microstructure such as V_f has an important influence on homogenized results.

Relationship between the randomness of $\boldsymbol{\alpha}^{EI}$ and V_f is investigated under different correlative conditions by RFM and MCM when all micro-structural parameters are random. In this section, the coefficient of variance of every random parameter is still 0.05, and ρ means $\rho_{e_m v_m} = \rho_{e_f v_f} = \rho_{a_1 a_2}$.

Coefficient of variance $\gamma_{\alpha^{EI}}$ of $\boldsymbol{\alpha}^{EI}$ is firstly given in Table 7 and illustrated in Fig. 5. Results show that coefficients of variance of elements α_1 and α_2 increase while that of element α_3 decreases with the increasing V_f no matter random micro-structural parameters are correlative or not correlative. Again, the conclusions from section 3.2 are verified: with the increasing ρ, the randomness of α_1 and α_2 decreases while that of α_3 increases slightly.

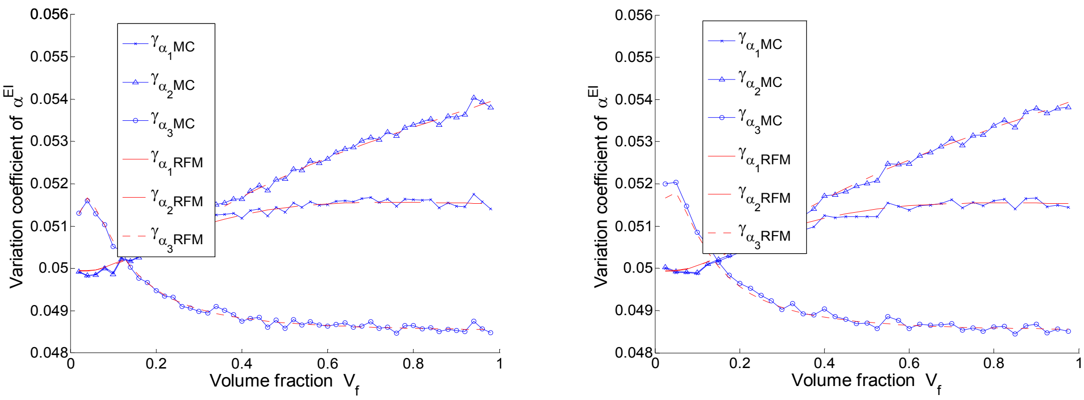

Fig. 5 Variation coefficient of $\boldsymbol{\alpha}^{EI}$ when $\rho_{e_m v_m} = \rho_{e_f v_f} = \rho_{a_1 a_2}$ =0 (left) and that when $\rho_{e_m v_m} = \rho_{e_f v_f} = \rho_{a_1 a_2}$=0.8 (right)

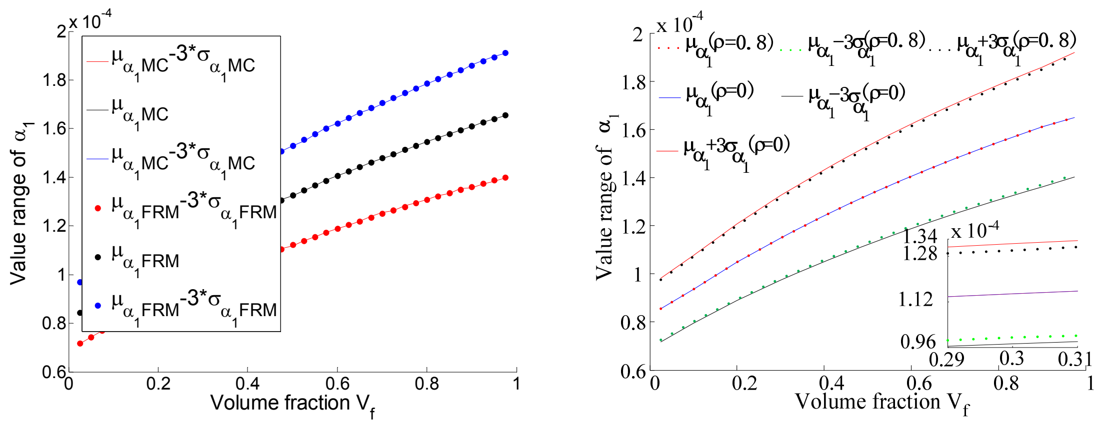

Fig. 6 Value range of element α_1 given by two methods (left) and that of α_1 given under different correlative conditions (right)

The mean value $\mu_{\alpha^{EI}}$, upper bound $\mu_{\alpha^{EI}} + 3\sigma_{\alpha^{EI}}$ and lower bound $\mu_{\alpha^{EI}} - 3\sigma_{\alpha^{EI}}$ of $\boldsymbol{\alpha}^{EI}$ are given in Figs. 6-7, which illustrate the value range of $\boldsymbol{\alpha}^{EI}$ according to $\pm 3\sigma$ rule.

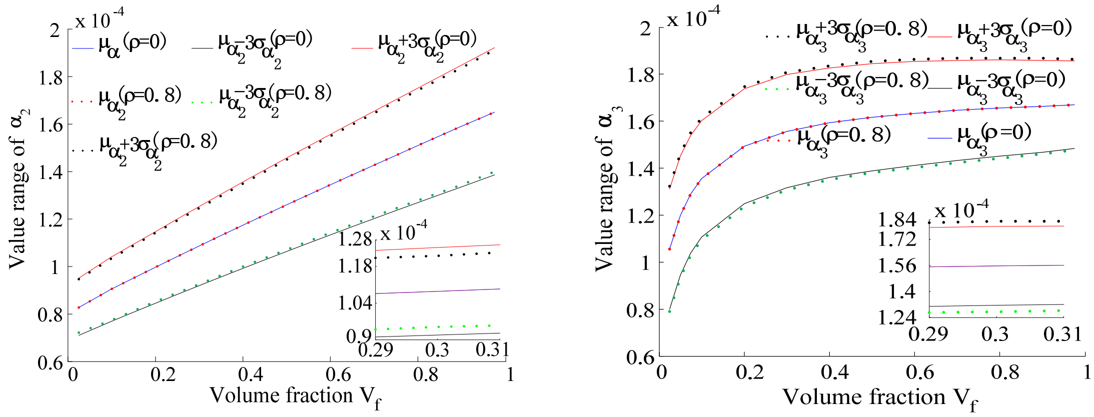

Fig. 7 Value range of α_2 (left) and of α_3 (right) given under different correlative conditions

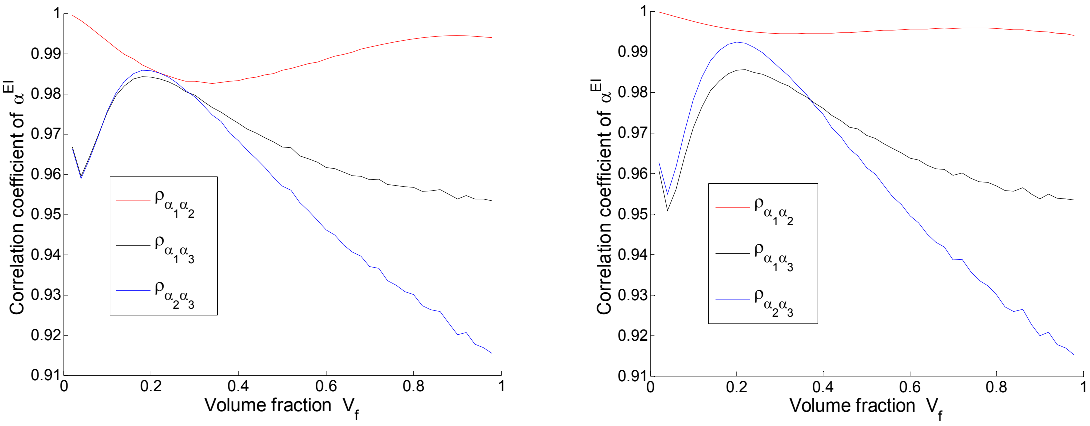

Fig. 8 Correlative curves of $\boldsymbol{\alpha}^{EI}$ when $\rho_{e_m v_m} = \rho_{e_f v_f} = \rho_{a_1 a_2}$=0 (left) and $\rho_{e_m v_m} = \rho_{e_f v_f} = \rho_{a_1 a_2}$=0.8 (right)

From Figs. 6-7, values of $\mu_{\alpha^{EI}}$, $\mu_{\alpha^{EI}} + 3\sigma_{\alpha^{EI}}$ and $\mu_{\alpha^{EI}} - 3\sigma_{\alpha^{EI}}$ augment with the increasing V_f. Moreover, the difference $6\sigma_{\alpha^{EI}}$ of upper bound $\mu_{\alpha^{EI}} + 3\sigma_{\alpha^{EI}}$ and $\mu_{\alpha^{EI}} - 3\sigma_{\alpha^{EI}}$ for α_1 and α_2 enlarges with the increasing V_f while that for α_3 slightly decrease, which is consistent with the conclusions summarized from Fig. 5 and Table 7. In addition, the value range of α_1 or α_2 for ρ=0.8 is comprised by that for ρ=0, as for α_3, the opposite is true, which is consistent with the conclusions obtained in section 3.2.

3.4 Impacts of different factors on the correlation among elements of $\boldsymbol{\alpha}^{EI}$

When fully considering the randomness of all parameters and the correlation among them, the correlation among elements of $\boldsymbol{\alpha}^{EI}$ is inspected by MCM, whereby coefficient of variance of every random parameter is still 0.05. The variation of correlation in $\boldsymbol{\alpha}^{EI}$ with V_f is shown in Fig. 8 under different correlative cases.

From Fig. 8, the curves of correlation coefficients $\rho_{\alpha_1\alpha_2}$ and $\rho_{\alpha_1\alpha_3}$ as well as $\rho_{\alpha_2\alpha_3}$ for $\rho_{e_m v_m} = \rho_{e_f v_f} = \rho_{a_1 a_2}$=0.8 are different from that for $\rho_{e_m v_m} = \rho_{e_f v_f} = \rho_{a_1 a_2}$=0, that is, the correlation

Table 8 Correlation coefficients among elements of α^{EI} when V_f=0.25 (MCE: 10000)

	$\rho_{e_m v_m}$=0.1 $\rho_{e_f v_f}$=0.1 $\rho_{a_1 a_2}$=0.1	$\rho_{e_m v_m}$=0.5 $\rho_{e_f v_f}$=0.1 $\rho_{a_1 a_2}$=0.1	$\rho_{e_m v_m}$=0.1 $\rho_{e_f v_f}$=0.5 $\rho_{a_1 a_2}$=0.1	$\rho_{e_m v_m}$=0.1 $\rho_{e_f v_f}$=0.1 $\rho_{a_1 a_2}$=0.5	$\rho_{e_m v_m}$=0.5 $\rho_{e_f v_f}$=0.5 $\rho_{a_1 a_2}$=0.1	$\rho_{e_m v_m}$=0.1 $\rho_{e_f v_f}$=0.5 $\rho_{a_1 a_2}$=0.5	$\rho_{e_m v_m}$=0.5 $\rho_{e_f v_f}$=0.5 $\rho_{a_1 a_2}$=0.5	$\rho_{e_m v_m}$=0.9 $\rho_{e_f v_f}$=0.9 $\rho_{a_1 a_2}$=0.9	$\rho_{e_m v_m}$=1 $\rho_{e_f v_f}$=1 $\rho_{a_1 a_2}$=1
$\rho_{\alpha_1 \alpha_2}$	0.9854	0.9856	0.9855	0.9906	0.9856	0.9906	0.9907	0.9962	0.9979
$\rho_{\alpha_1 \alpha_3}$	0.9829	0.9826	0.9827	0.9846	0.9825	0.9846	0.9844	0.9854	0.9858
$\rho_{\alpha_2 \alpha_3}$	0.9845	0.9862	0.9853	0.9854	0.9870	0.9854	0.9862	0.9914	0.9923

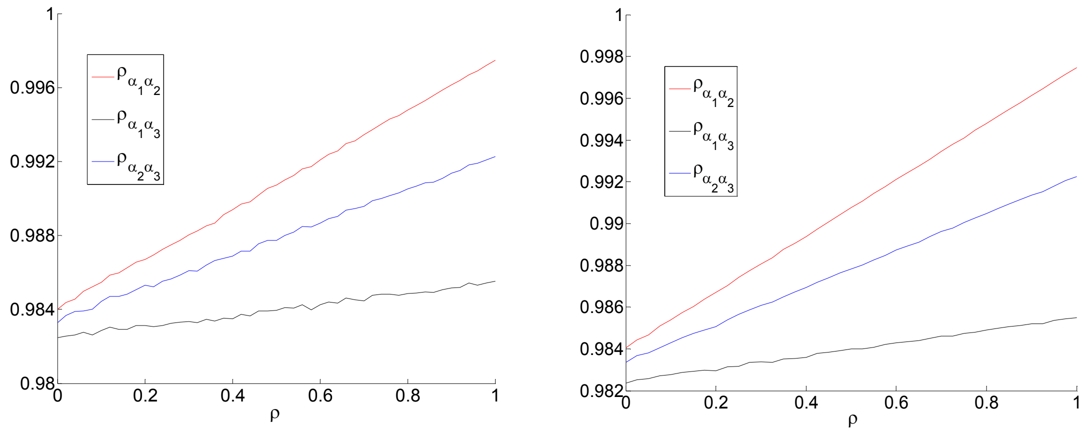

Fig. 9 Correlative curves of $\boldsymbol{\alpha}^{EI}$ with different number of realization (MCM: 5000 left and MCM: 50000 right)

among random parameters has obvious effects on the correlation among the homogenized results. Moreover, the correlation in $\boldsymbol{\alpha}^{EI}$ changes with the increasing V_f, and the greatest change is from $\rho_{\alpha_2\alpha_3}$ and is close to 10%.

When coefficient of variance of every variable is 0.05, correlation coefficients of $\boldsymbol{\alpha}^{EI}$ are listed in Table 8, and the correlative curves of $\boldsymbol{\alpha}^{EI}$ are illustrated in Fig. 9 as well.

From Fig. 9 and Table 8, it can be seen that elements α_1 and α_2 as well as α_3 exhibit very strong positive correlation that varies from 0.98 to 1.0 no matter the correlation among parameters is strong or weak. The correlation among $\boldsymbol{\alpha}^{EI}$ goes up with the increasing correlation of parameters, which reflects the correlation of parameters has a positive and direct effect on that of $\boldsymbol{\alpha}^{EI}$.

In order to demonstrate the impact of the correlation of parameters on that of $\boldsymbol{\alpha}^{EI}$, mean values of $\boldsymbol{\alpha}^{EI}$ are listed in Table 9 and indicated in Fig. 10 when $\gamma_{e_m}=\gamma_{v_m}=\gamma_{e_f}=\gamma_{v_f}=\gamma_{V_f}=\gamma_{a_1}=\gamma_{a_2}=\gamma_{\alpha_m}=\gamma_{\alpha_f}$=0.05 and V_f=0.25. Here ρ means $\rho_{e_m v_m}=\rho_{e_f v_f}=\rho_{a_1 a_2}$. The number of realization is 10000.

From Table 9 and Fig. 10, when ρ=1, $\rho_{\alpha_1\alpha_2}$ and $\rho_{\alpha_2\alpha_3}$ are nearly equal to 1 as shown in Table 8, so the distribution of red points corresponding to mean values of α_1 and α_2, α_2 and α_3 are very concentrated and almost in a straight line especially for 100 samples' realization, and predictably, such a trend is more obvious with the increasing number of samples' realization. Clearly, the correlation among $\boldsymbol{\alpha}^{EI}$ enlarges with the strengthening correlation of parameters.

Table 9 Mean values of elements of $\boldsymbol{\alpha}^{EI}$ computed from 10 samples of each random parameter (MCM: 10000)

ρ=0			ρ=0.5			ρ=1		
α_1 ($\times10^{-4}$)	α_2 ($\times10^{-4}$)	α_3 ($\times10^{-4}$)	α_1 ($\times10^{-4}$)	α_2 ($\times10^{-4}$)	α_3 ($\times10^{-4}$)	α_1 ($\times10^{-4}$)	α_2 ($\times10^{-4}$)	α_3 ($\times10^{-4}$)
1.0604	1.0046	1.4602	1.0597	1.0032	1.4598	1.0559	0.9981	1.4578
1.1007	1.0310	1.5049	1.1009	1.0273	1.4986	1.1025	1.0356	1.5121
1.1375	1.0619	1.5879	1.1373	1.0693	1.5903	1.1343	1.0828	1.5926
1.1863	1.1112	1.6298	1.1846	1.1116	1.6295	1.1797	1.1153	1.6295
1.1671	1.1037	1.6343	1.1686	1.1033	1.6345	1.1706	1.1091	1.6373
1.1067	1.0596	1.5527	1.1080	1.0624	1.5535	1.1131	1.0597	1.5536
1.0293	0.9712	1.4281	1.0294	0.9726	1.4285	1.0274	0.9747	1.4287
1.0557	0.9919	1.4664	1.0549	0.9926	1.4665	1.0557	0.9982	1.4696
1.0462	0.9813	1.4325	1.0433	0.9756	1.4254	1.0407	0.9730	1.4190
1.2070	1.1367	1.6639	1.2049	1.1317	1.6568	1.2062	1.1317	1.6568

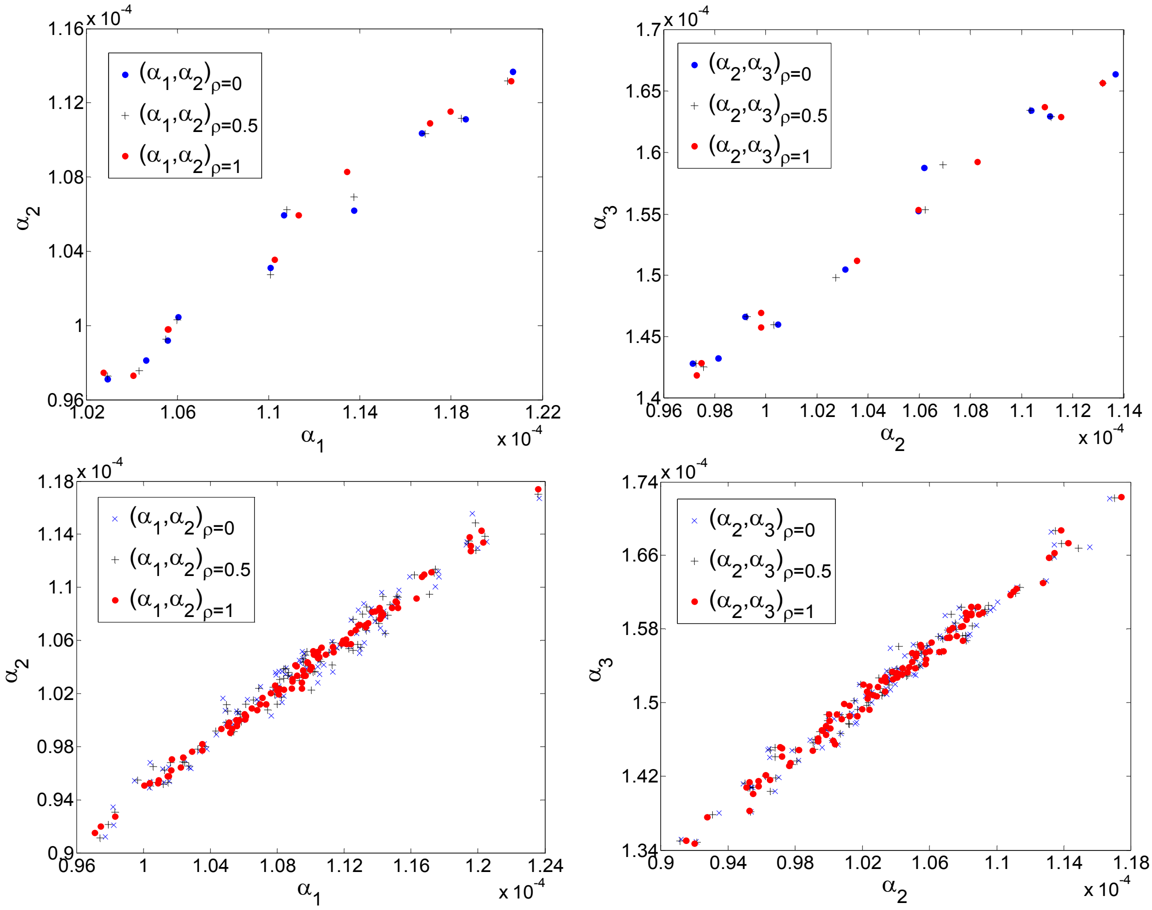

Fig. 10 Results obtained from 10 samples of every parameter (above) and that obtained from 100 samples of each parameter (below)

4. Conclusions

The subject of stochastic homogenization is devoted to the determination of the properties of a homogeneous material that approximates the behavior of the original heterogeneous problem with uncertainty. This work focuses on stochastic homogenization of a fiber reinforced composite material with uncertainty in microstructure, and the target is to address the relationship between the micro-structural uncertainty including the full randomness and correlation and the uncertainty of macroscopic thermal properties. In order to demonstrate such uncertainty existing in homogenized results, numerical characteristics such as the mean value and mean square deviation as well as coefficient of variance together with correlation coefficient of effective thermal expansion coefficient tensor are derived, which is quite crucial for the application in engineering, e.g. reliability analysis of structure comprising such composites bearing thermal stresses.

This work focuses in particular on the evaluation of the macroscopic thermal expansion coefficient tensor based on the analytical Mori-Tanaka estimate, in presence of uncertainties of the geometry and material parameters of the microstructure. Results from RFM are compared with those from the Monte-Carlo Method (MCM) simulations in order to validate the proposed method.

From the numerical results, the following conclusions can be obtained:

• The sets of numerical results from the RFM and the MCM are in very good agreement. Hence the proposed method delivers the same accuracy of the MCM with lower computational cost;

• The random effective thermal expansion coefficient tensor elements are significantly affected not only by the randomness of the micro-structural parameters but also by their correlation. The impacts of all random parameters on the randomness of $\boldsymbol{\alpha}^{EI}$ are complementary and interactive;

• Different random parameters and their correlation have different impacts on the random effective thermal expansion coefficient tensor;

• The correlation among random micro-structural parameters not only impacts the randomness of the effective thermal expansion coefficient tensor elements but also affects their value ranges and their correlation. The correlation among $\boldsymbol{\alpha}^{EI}$ remains very high and goes up with the increasing correlation among random parameters;

• The randomness of V_f significantly affects the randomness and the correlation of effective thermal expansion coefficient tensor elements. Variation coefficients γ_{α_1} and γ_{α_2} increase while γ_{α_3} decreases with the increasing V_f, which directly determines the enlarging difference of upper and lower bounds of α_1 or α_2 and the decreasing difference of α_3 with the augment of V_f.

As for two methods used for random homogenization here, the oscillation of results from RFM is much smaller than that from MCM as shown in Fig. 5, which is because MCM significantly depends on the realization number as illustrated in Fig. 9. RFM needs much less computational cost than MCM but outputs results with comparable accuracy to MCM. As shown in this paper, whenever an explicit relationship is available between homogenized results and micro-structural parameters, regardless whether this relationship is linear or nonlinear, the random homogenized results can be easily evaluated by the RFM.

Moreover, the content of this work is analytical, although the wide range of micromechanical problems can be tackled with robust numerical methods. As in many other engineering fields, it is not wrong to say that the computational methods available to analyze micromechanical problems have superseded analytical ones as well as those available via laboratory experiments. However, analytical tools are indispensible for a solid foundation for computational methods. In addition, the stochastic homogenized results from RFM and MCM are verified by each other and consistent with each other very well, which will be the robust basis for the stochastic homogenization problem based on computational techniques combined with the Monte-carlo method in the future work.

Acknowledgments

The first author gratefully acknowledges the support of the Alexander von Humboldt Stiftung through a 'Humboldt Research Fellowship for Postdoctoral Researchers' for a research stay at the Leibniz Universität Hannover. The support of Natural Science Foundation of China to the project (JJ0500110405) "Random homogenization of heterogeneous materials with infinitesimal and finite deformation" is also gratefully acknowledged.

References

Aboudi, J. (1991), *Mechanics of Composites Materials: A Unified Micromechanical Approach*, Elesevier, Amsterdam, Netherlands.

Ashida, F., Tauchert, T.R., Sakata, S. and Yamashita, Y. (2003), "Control of transient deformation in a heated intelligent composite disk", *Smart Mater. Struct.*, **12**(5), 825-35.

Bris, C.L. (2010), *Numerical Mathematics and Advanced Applications 2009*, Springer, Heidburg, Germany.

Eshelby, J.D. (1957), "The elastic field of an ellipsoidal inclusion, and related problems", *Proc. Roy. Soc. A*, **241**, 376-396.

Gao, W., Chen, J.J., Ma, J. and Liang, Z.T. (2004), "Dynamic response analysis of stochastic frame structures under nonstationary random excitation", *AIAA J.*, **42**(9), 1818-1822.

Hashin, Z. and Shtrikman, S. (1962), "On some variational principles in anisotropic and nonhomogeneous elasticity", *J. Mech. Phys. Solid.*, **10**, 335-342.

Hiriyur, B., Waisman, H. and Deodatis, G. (2011), "Uncertainty quantification in homogenization of heterogeneous microstructures modeled by XFEM", *Int. J. Numer. Meth. Eng.*, **88**(3), 257-278.

Knott, G.M., Jackson, T.L. and Buckmaster, J. (2011), "Random packing of heterogeneous propellants", *AIAA J.*, **39**(4), 678-686.

Lascoup, B., Perez, L. and Autriaue, L. (2013), "On the feasibility of defect detection in composite material based on thermal periodic excitation", *Compos. Part B-Eng.*, **45**(1), 1023-1030.

Li, J. (1993), "Some trends of structural dynamic analysis", *World Earthq. Eng.*, **2**, 1-8. (in Chinese)

Li, X.X. (1991), "Spatial random response analysis and damage assessment of multi storey reinforced concrete structure under strong earthquake excitation", Ph.D. Dissertation, Southwest Jiaotong University, Chengdu. (in Chinese)

Lu, Z.X., Yuan, Z.S. and Liu, Q. (2013), "3D numerical simulation for the elastic properties of random fiber composites with a wide range of fiber aspect ratios", *Comp. Mater. Sci.*, **90**, 123-129.

Ma, J., Wriggers, P., Gao, W., Chen, J.J. and Sahraee, S. (2011), "Reliability-based optimization of trusses with random parameters under dynamic loads", *Comp. Mech.*, **47**, 627-640.

Miehe, C., Schotte, J. and Schröder, J. (1999), "Computational micromacro transitions and overall moduli in the analysis of polycrystals at large strains", *Comp. Mater. Sci*., **16**, 372-382.

Mori, T. and Tanaka, K. (1972), "Average stress in matrix and average elastic energy of materials with misfitting inclusions", *Acta Metall*, **21**, 571-574.

Nemat-Nasser, S. and Hori, M. (1999), *Micromechanics: Overall Properties of Heterogeneous Solids*, Elsevier, Amsterdam, Netherlands.

Reuss, A. (1929), "Berechnung der fliessgrenz von mischkristallen auf grund der plastizitatsbedingung fur einkristalle. Z. Angew", *Math. Mech. Solid.*, **9**, 49-58.

Rong, J.L., Gan, Z.K. and Wang, D. (2015), "Numerical predictions of the mechanical properties of

NT-ZnOw reinforced composites", *Comp. Mater. Sci*., **96**, 185-190.
Sakata, S., Ashida, F. and Kojima, T. (2008), "Stochastic homogenization analysis on elastic properties of fiber reinforced composites using the equivalent inclusion method and perturbation method", *Int. J. Solid. Struct.*, **45**(25-26), 6553-6565.
Stroeven, M., Askes, H. and Sluys, L. J. (2004), "Numerical determination of representative volumes for granular materials", *Comput. Meth. Appl. M.*, **193**, 3221-3238.
Takao, Y. and Taya, M. (1985), "Thermal expansion coefficients and thermal stresses in an aligned short fiber composite with application to a short carbon fiber/aluminum", *J. Appl. Mech.*, **52**(4), 806-810.
Tian, W.L., Qi, L.H. and Zhou, J.M. (2015), "Quantitative characterization of the fiber orientation variation in the Csf/Mg composites", *Comp. Mater. Sci*., **98**, 56-63.
Tohgo, K. (2004), *Analysis of material strength*, Uchida Rokakuho, Japan.
Tootkaboni, M. and Graham-Brady, L. (2010), "A multi-scale spectral stochastic method for homogenization of multi-phase periodic composites with random material properties", *Int. J. Numer. Meth. Eng.*, **83**(1), 59-90.
Torquato, S. (2002), *Random Heterogeneous Materials: Microstructure and Macroscopic Properties*, Springer, Heidburg, Germany.
Touran, A. and Wiser, E.P. (1992), "Monte Carlo technique with correlated random variables", *J. Constr. Eng. M.*, **118**, 258-272.
Vel, S.S. and Goupee, A.J. (2010), "Multiscale thermoelastic analysis of random heterogeneous materials: Part I: Microstructure characterization and homogenization of material properties", *Comp. Mater. Sci*., **48**(1), 22-38.
Voigt, W. (1889), "Uber die beziehung zwischen den beiden elastizitatskonstanten isotroper korper", *Wied. Ann.*, **38**, 573-587.
Wu, T., Temizer, I. and Wriggers, P. (2014), "Multiscale hydro-thermo-chemo-mechanical coupling: application to alkali-silica reaction", *Comp. Mater. Sci*., **84**, 381-395.
Xu, X.F. and Stefanou, G. (2012), "Explicit bounds on elastic moduli of solids containing isotropic mixture of cracks and voids", *Fatig. Fract. Eng. M.*, **35**(8), 708-717.
Zohdi, T. and Wriggers, P. (2008), *An Introduction to Computational Micromechanics*, Springer, Berlin, Heidelberg, New York, Germany.

CC

Appendix

$$\frac{\partial \boldsymbol{\alpha}^{EI}}{\partial e_m} = V_f \boldsymbol{A}^{-1}[\frac{\partial \boldsymbol{D}^{-1}}{\partial e_m}\boldsymbol{\beta}\boldsymbol{E}_f + \boldsymbol{D}^{-1}\frac{\partial \boldsymbol{\beta}}{\partial e_m}\boldsymbol{E}_f]\boldsymbol{\varphi} \tag{1}$$

$$\frac{\partial \boldsymbol{\alpha}^{EI}}{\partial e_f} = V_f \{\boldsymbol{A}^{-1}[\frac{\partial \boldsymbol{D}^{-1}}{\partial e_f}\boldsymbol{\beta}\boldsymbol{E}_f + \boldsymbol{D}^{-1}\frac{\partial \boldsymbol{\beta}}{\partial e_f}\boldsymbol{E}_f + \boldsymbol{D}^{-1}\boldsymbol{\beta}\frac{\partial \boldsymbol{E}_f}{\partial e_f}]\boldsymbol{\varphi}\} \tag{2}$$

$$\frac{\partial \boldsymbol{\alpha}^{EI}}{\partial \nu_f} = V_f \{\frac{\partial \boldsymbol{A}^{-1}}{\partial \nu_{\mathrm{f}}}[\boldsymbol{D}^{-1}\boldsymbol{\beta}\boldsymbol{E}_f - \boldsymbol{A}]\ \boldsymbol{\varphi} + \boldsymbol{A}^{-1}[\frac{\partial \boldsymbol{D}^{-1}}{\partial \nu_f}\boldsymbol{\beta}\boldsymbol{E}_f + \boldsymbol{D}^{-1}\frac{\partial \boldsymbol{\beta}}{\partial \nu_f}\boldsymbol{E}_f + \boldsymbol{D}^{-1}\beta\frac{\partial \boldsymbol{E}_f}{\partial \nu_f} - \frac{\partial \boldsymbol{A}}{\partial \nu_f}]\ \boldsymbol{\varphi}\} \tag{3}$$

$$\frac{\partial \boldsymbol{\alpha}^{EI}}{\partial V_f} = \{\boldsymbol{A}^{-1}[\boldsymbol{D}^{-1}\boldsymbol{\beta}\boldsymbol{E}_f - \boldsymbol{A}]\boldsymbol{\varphi}\} + V_f \{\frac{\partial \boldsymbol{A}^{-1}}{\partial V_f}[\boldsymbol{D}^{-1}\boldsymbol{\beta}\boldsymbol{E}_f - \boldsymbol{A}]\boldsymbol{\varphi} + \boldsymbol{A}^{-1}[\frac{\partial \boldsymbol{D}^{-1}}{\partial V_f}\boldsymbol{\beta}\boldsymbol{E}_f + \boldsymbol{D}^{-1}\frac{\partial \boldsymbol{\beta}}{\partial V_f}\boldsymbol{E}_f - \frac{\partial \boldsymbol{A}}{\partial V_f}]\boldsymbol{\varphi}\} \tag{4}$$

$$\frac{\partial \boldsymbol{\alpha}^{EI}}{\partial a_1} = V_f \{\frac{\partial \boldsymbol{A}^{-1}}{\partial a_1}[\boldsymbol{D}^{-1}\boldsymbol{\beta}\boldsymbol{E}_f - \boldsymbol{A}]\boldsymbol{\varphi} + \boldsymbol{A}^{-1}[\frac{\partial \boldsymbol{D}^{-1}}{\partial a_1}\boldsymbol{\beta}\boldsymbol{E}_f + \boldsymbol{D}^{-1}\frac{\partial \boldsymbol{\beta}}{\partial a_1}\boldsymbol{E}_f - \frac{\partial \boldsymbol{A}}{\partial a_1}]\boldsymbol{\varphi}\} \tag{5}$$

$$\frac{\partial \boldsymbol{\alpha}^{EI}}{\partial a_2} = V_f \{\frac{\partial \boldsymbol{A}^{-1}}{\partial a_2}[\boldsymbol{D}^{-1}\boldsymbol{\beta}\boldsymbol{E}_f - \boldsymbol{A}]\boldsymbol{\varphi} + \boldsymbol{A}^{-1}[\frac{\partial \boldsymbol{D}^{-1}}{\partial a_2}\boldsymbol{\beta}\boldsymbol{E}_f + \boldsymbol{D}^{-1}\frac{\partial \boldsymbol{\beta}}{\partial a_2}\boldsymbol{E}_f - \frac{\partial \boldsymbol{A}}{\partial a_2}]\boldsymbol{\varphi}\} \tag{6}$$

$$\frac{\partial \boldsymbol{\alpha}^{EI}}{\partial \alpha_m} = \boldsymbol{I} + V_f \{\boldsymbol{A}^{-1}[\boldsymbol{D}^{-1}\boldsymbol{\beta}\boldsymbol{E}_f - \boldsymbol{A}] + \boldsymbol{I}\}\ \frac{\partial \boldsymbol{\varphi}}{\partial \alpha_m} \tag{7}$$

$$\frac{\partial \boldsymbol{\alpha}^{EI}}{\partial \alpha_f} = V_f \{\boldsymbol{A}^{-1}[\boldsymbol{D}^{-1}\boldsymbol{\beta}\boldsymbol{E}_f - \boldsymbol{A}] + \boldsymbol{I}\}\ \frac{\partial \boldsymbol{\varphi}}{\partial \alpha_f} \tag{8}$$